

Bulk properties of QCD matter from lattice simulations

Claudia Ratti

Department of Physics, University of Houston, Houston, TX 77204, USA

E-mail: cratti@uh.edu

Abstract. A review of the most recent results on QCD thermodynamics, obtained from lattice simulations, is presented. Particular focus is devoted to fluctuations of conserved charges and to their comparison with the experimental results from RHIC Beam Energy Scan.

1. Introduction

The deconfined phase of Quantum Chromodynamics (QCD), the Quark-Gluon Plasma (QGP) can be created in the laboratory in heavy ion collision experiments currently running at RHIC (Brookhaven National Laboratory) and at the LHC (CERN). These experiments allow to explore the QCD phase diagram and to extract the properties of this new phase of matter. The QGP turns out to be the most ideal fluid ever observed, which led to the idea that the system created in the collisions is strongly interacting and cannot be studied by means of perturbative techniques.

Lattice simulations are the best first-principle tool to address QCD in its non-perturbative regime. Given enough computer power, both statistical and systematic uncertainties can be kept under control. Due to a steady and continuous improvement in computer resources, numerical algorithms and our physical understanding which manifests itself in physical techniques (e.g. the Wilson-flow scale setting introduced in Ref. [1]), the lattice results which are being produced today reach an unprecedented level of accuracy, which allows a quantitative comparison to experimental observables for the first time.

The region of the phase diagram which can be explored experimentally corresponds to values of temperature T and chemical potential μ_B for which perturbative techniques are not applicable: this endorses lattice QCD as the main tool to investigate the properties of the matter created in heavy ion collisions. In the low temperature phase, interacting hadronic matter in the ground state can be well described in terms of a gas of non-interacting hadrons and resonances. Indeed the Hadron Resonance Gas (HRG) model, based on this idea, yields a very good description of the lattice results for QCD thermodynamics.

The availability of precise experimental data, as well as the accuracy of the lattice QCD results, allows a new synergy between fundamental theory and experiment, which leads to the determination of several properties of the QGP from first principles.

2. QCD equation of state

The QCD equation of state at zero chemical potential is now known with high accuracy: continuum extrapolated results are available for the pressure, energy density, entropy density,

interaction measure and speed of sound of a system of 2+1 quark flavors with physical quark masses [2, 3, 4]. A selection of these results is shown in the left panel of Fig. 1, in which curves from the WB collaboration obtained with the 2stout action (gray) are compared to those from the HotQCD collaboration obtained with the HISQ action (colored). The agreement between the two sets of curves is a fundamental test of the validity of the lattice approach to solve QCD.

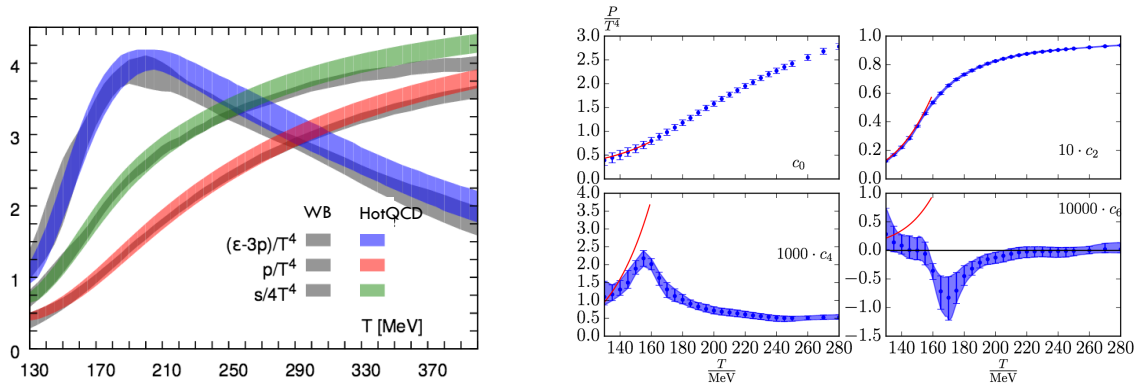


Figure 1. Left: Scaled pressure, entropy density and interaction measure as functions of the temperature. The gray curves have been obtained by the WB collaboration with the 2stout action [2, 3], the colored ones by the HotQCD collaboration with the HISQ action [4]. Right: Taylor coefficients c_0 , c_2 , c_4 and c_6 as functions of the temperature from the WB collaboration, obtained from imaginary μ_B simulations. The data are continuum extrapolated [14, 15, 16].

Lattice QCD simulations at finite chemical potential are unfortunately not possible, due to the sign problem. Different methods have been proposed in order to circumvent the problem: here I will focus on the Taylor expansion of thermodynamic observables around $\mu_B = 0$ [5, 6] (which can be considered as a truncated version of the multiparameter reweighting technique [7]) and on the analytical continuation from imaginary chemical potentials [8, 9, 10].

The Taylor expansion of the pressure in powers of μ_B/T can be written as:

$$\frac{p(\mu_B)}{T^4} = c_0(T) + c_2(T) \left(\frac{\mu_B}{T}\right)^2 + c_4(T) \left(\frac{\mu_B}{T}\right)^4 + c_6(T) \left(\frac{\mu_B}{T}\right)^6 + \mathcal{O}(\mu_B^8). \quad (1)$$

The coefficients $c_i(T)$ in the above expansion can be calculated on the lattice. Several results exist in the literature: $c_2 \dots c_6$ have been calculated long ago on coarse lattices and with heavier than physical quark masses [11]; continuum extrapolated results for c_2 at the physical quark mass were published for the first time in Ref. [12]; results for c_4 at finite lattice spacing were shown in Ref. [13]. In Fig. 1 right I show the new results for c_2 , c_4 and c_6 from the WB collaboration, in the continuum limit and for physical quark masses. These results have been obtained with the method of analytical continuation from imaginary chemical potential [14, 15, 16]. It is important to notice that the chemical potentials μ_B , μ_S and μ_Q are not independent of each other: μ_S and μ_Q are both functions of T and μ_B , such that the following experimental conditions are satisfied:

$$\rho_S = 0, \quad \rho_Q = 0.4\rho_B, \quad (2)$$

where ρ_S , ρ_Q and ρ_B are the densities of strangeness, charge and baryonic number, respectively. The coefficients $c_2 \dots c_6$ in Eq. (1) are full derivatives with respect to μ_B/T , namely they take into account the dependence of μ_S and μ_Q on μ_B and T .

3. QCD phase diagram

It is known from lattice QCD simulations that the deconfinement transition at $\mu_B = 0$ is an analytical crossover [17], taking place over a broad range of temperatures around $T_c \simeq 155$ MeV [18, 19, 20, 21]. The transition temperature is usually defined by locating the inflection point of relevant observables. As the chemical potential is increased, the position of the inflection point changes: it is possible to express the μ_B -dependence of T_c in the following way:

$$\frac{T_c(\mu_B)}{T_c(\mu_B = 0)} = 1 - \kappa \left(\frac{\mu_B}{T_c(\mu_B)} \right)^2 + \lambda \left(\frac{\mu_B}{T_c(\mu_B)} \right)^4 + \dots \quad (3)$$

The coefficient κ is the curvature of the phase diagram. By looking at the chiral condensate, chiral susceptibility and strange quark susceptibility the WB collaboration finds a value of $\kappa = 0.0149 \pm 0.0021$ [22]; the strange quark chemical potential is fixed to impose strangeness neutrality. The phase diagram corresponding to this value of κ is showed in the left panel of Fig. 2, together with a compilation of freeze-out parameters obtained with different methods. The shaded band indicates the broadness of the QCD transition, while the dark blue band shows that it is possible to find a value for T_c with great accuracy when looking at a single observable (in this case the chiral condensate). Similar results have been obtained recently by two other groups: P. Cea *et al.* obtain a value of $\kappa = 0.020(4)$ by fixing $\mu_s = \mu_l$ [23], while Bonati *et al.* find $\kappa = 0.0135(20)$ both with $\mu_s = 0$ and $\mu_s = \mu_l$ [24]. In the right panel of Fig. 2, the phase diagram with the curvature from Ref. [23] is shown.

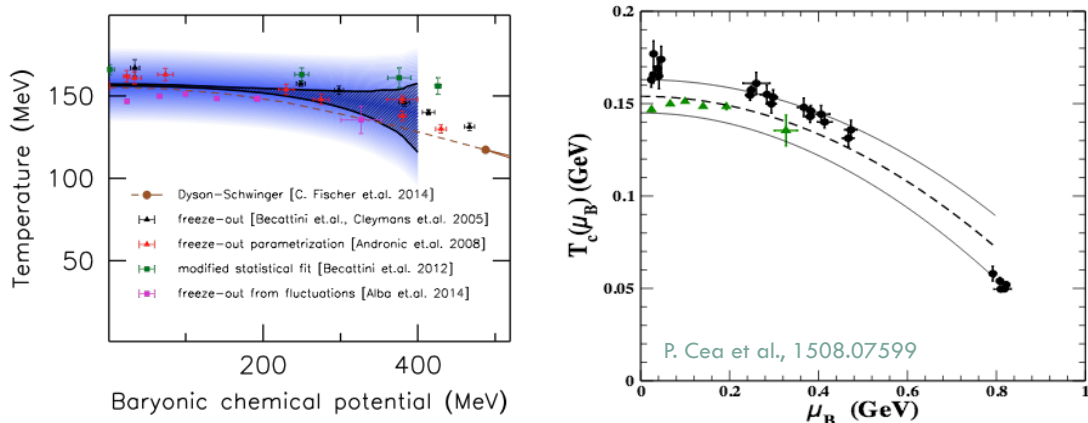


Figure 2. Left: The phase diagram based on the μ_B -dependent T_c from the chiral condensate, analytically continued from imaginary chemical potential [22]. The blue band indicates the width of the transition. The shaded black region shows the transition line obtained from the chiral condensate. The widening around 300 MeV is coming from the uncertainty of the curvature and from the contribution of higher order terms, thus the application range of the results is restricted to smaller values. We also show some selected non-lattice results: the Dyson-Schwinger result [25], and the freeze-out data of Refs. [26]-[32]. Right: analogous plot from Ref. [23].

4. Fluctuations of conserved charges

Fluctuations of conserved charges are the most prominent example of direct comparison between lattice QCD results and experimental data: they are fixed at the chemical freeze-out, therefore they can be used to gain information about this point in the evolution of a heavy ion collision [33, 34].

The definition of fluctuations is as follows:

$$\chi_{lmn}^{BQS}(T, \mu_B) = \frac{\partial^{l+m+n} p/T^4}{\partial(\mu_B/T)^l \partial(\mu_Q/T)^m \partial(\mu_S/T)^n} \quad (4)$$

and they can be related to the cumulants of the event by event distribution of the corresponding net conserved charge measured in experiments. In particular, it is possible to define volume-independent ratios which only depend on T and μ_B :

$$\begin{aligned} M/\sigma^2 &= \chi_1/\chi_2 & S\sigma^3/M &= \chi_3/\chi_1 \\ S\sigma &= \chi_3/\chi_2 & \kappa\sigma^2 &= \chi_4/\chi_2 \end{aligned} \quad (5)$$

where M is the mean of the experimental distribution, σ the variance, S the skewness and κ the kurtosis. The lattice QCD results for the above ratios will depend on T and μ_B : by comparing them to the experimental value it is therefore possible to extract the freeze-out temperature and chemical potential.

In the comparison between a first principle calculation in thermal equilibrium and the data from a heavy ion collision, we have to make sure that the experiment is measuring thermal fluctuations as well, and that other spurious sources of fluctuations are under control. The system created in a heavy ion collision is a canonical ensemble, in which charges like baryon number or electric charge are strictly conserved. However, if we look at a limited part of this system (which can be done due to the limited acceptance of the detector), we can treat it as a Grand Canonical Ensemble [35]. There are several effects which may generate non-thermal fluctuations: fluctuations in the initial volume, protons coming from the interaction with the beam pipe, effects due to cuts in rapidity and transverse momentum, and so on. A variety of effects has been identified and studied in the literature [36]-[42].

The WB collaboration showed that, by analyzing the fluctuations of electric charge and baryon numbers separately [44, 45], a consistency is found in the chemical freeze-out μ_B values [43], with the freeze-out temperature having an upper limit of $T_{ch} \leq 151 \pm 4$ MeV. More recently, the authors of Ref. [46] were able to obtain both the freeze-out temperature and the curvature of the freeze-out line. The value of the freeze-out temperature ($T_f = (147 \pm 2)$ MeV) is in agreement with the one obtained in Ref. [43]. The WB collaboration performed a combined fit of χ_1/χ_2 for electric charge and proton number and found the freeze-out temperature and chemical potential for the highest RHIC energies. These preliminary results are shown in the left panel of Fig. 3, together with the isentropic lines which match the freeze-out data, the contours for constant mean/variance of net-electric charge and net-baryon number from the lattice, and the results of a previous analysis based on the HRG model [32].

Strangeness is still missing from the picture mainly due to the lack of experimental data for the fluctuations of (multi-)strange baryons. Therefore, it is important to have a first-principle determination of the strangeness freeze-out temperature. The ALICE data for particle yields and ratios seem to indicate a tension between the freeze-out temperatures in the light and strange sectors [48, 49]. Several explanations have been proposed for this result [50]-[57], but so far none has been validated or excluded. A result from first principles would finally resolve this issue.

So far, the only feasible experimental measurement of fluctuations of strange particles is the net-kaon fluctuations, which will be finalized soon by the STAR collaboration. In Ref. [58] we showed that it is possible to isolate the kaon fluctuations in lattice QCD simulations: the experimental kaon distribution contains both primordial kaons and those produced by resonance decays. By using an HRG model with resonance decays, we showed that the χ_2/χ_1 of the full kaon distribution is effectively identical to the one obtained for primordial kaons in the Boltzmann approximation. The latter is given by a simple formula:

$$\frac{\chi_2^K}{\chi_1^K} = \frac{\cosh(\hat{\mu}_S + \hat{\mu}_Q)}{\sinh(\hat{\mu}_S + \hat{\mu}_Q)} \quad (6)$$

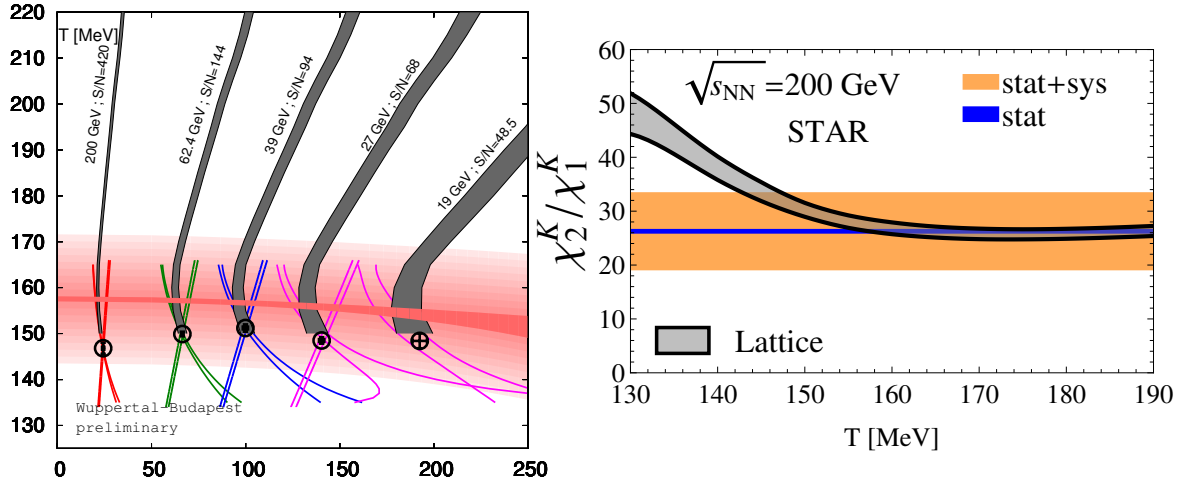


Figure 3. Left: Preliminary results for the freeze-out parameters from the WB collaboration. The colored full and dashed lines are the contours at constant mean/variance ratios of the net electric charge and net baryon number from lattice simulations. The contours that correspond to STAR data intersect in the freeze-out points of Ref. [32]. The red band is the QCD phase diagram shown in Fig. 2. Also shown are the isentropic contours that match the chemical freeze-out data [14, 15, 16]. Right: Example of comparison between χ_2^K / χ_1^K from lattice QCD and the preliminary STAR result at $\sqrt{s} = 200$ GeV shown at the Strangeness in Quark Matter 2016 conference [47]. The blue band corresponds to the statistical error, the orange one shows statistical and systematic errors summed in quadrature.

which can be easily calculated on the lattice. An example of lattice-to-experiment comparison for this observable is shown in the right panel of Fig. 3. When the STAR data for this observable are finalized, it will be possible to extract the freeze-out parameters for kaons from first principles.

5. Conclusions

In conclusion, lattice QCD simulation have reached a new level of accuracy in the last few years. Precise results are available for QCD thermodynamics at zero and small chemical potentials, which allow a quantitative comparison with experimental results for the first time. This will eventually enable us to achieve a comprehensive understanding of bulk properties of QCD matter from first principles.

Acknowledgements

This material is based upon work supported by the National Science Foundation under grant no. PHY-1513864 and by the U.S. Department of Energy, Office of Science, Office of Nuclear Physics, within the framework of the Beam Energy Scan Theory (BEST) Topical Collaboration. An award of computer time was provided by the INCITE program. This research used resources of the Argonne Leadership Computing Facility, which is a DOE Office of Science User Facility supported under Contract DE-AC02-06CH11357.

References

- [1] S. Borsanyi *et al.*, JHEP **1209** (2012) 010
- [2] S. Borsanyi *et al.*, JHEP **1011** (2010) 077
- [3] S. Borsanyi, Z. Fodor, C. Hoelbling, S. D. Katz, S. Krieg and K. K. Szabo, Phys. Lett. B **730** (2014) 99
- [4] A. Bazavov *et al.* [HotQCD Collaboration], Phys. Rev. D **90** (2014) 094503
- [5] C. R. Allton *et al.*, Phys. Rev. D **66** (2002) 074507

- [6] R. V. Gavai and S. Gupta, Phys. Rev. D **78** (2008) 114503
- [7] Z. Fodor and S. D. Katz, Phys. Lett. B **534** (2002) 87
- [8] P. de Forcrand and O. Philipsen, Nucl. Phys. B **642** (2002) 290
- [9] M. D'Elia and M. P. Lombardo, Phys. Rev. D **67** (2003) 014505
- [10] L. K. Wu, X. Q. Luo and H. S. Chen, Phys. Rev. D **76** (2007) 034505
- [11] C. R. Allton *et al.*, Phys. Rev. D **71** (2005) 054508
- [12] S. Borsanyi, G. Endrodi, Z. Fodor, S. D. Katz, S. Krieg, C. Ratti and K. K. Szabo, JHEP **1208** (2012) 053
- [13] P. Hegde [BNL-Bielefeld-CCNU Collaboration], Nucl. Phys. A **931**, 851 (2014)
- [14] R. Bellwied *et al.*, arXiv:1601.00466 [nucl-th].
- [15] C. Ratti, arXiv:1601.02367 [hep-lat].
- [16] J. Gunther, R. Bellwied, S. Borsanyi, Z. Fodor, S. Katz, A. Pasztor and C. Ratti, arXiv:1607.02493 [hep-lat].
- [17] Y. Aoki, G. Endrodi, Z. Fodor, S. D. Katz and K. K. Szabo, Nature **443** (2006) 675
- [18] Y. Aoki, Z. Fodor, S. D. Katz and K. K. Szabo, Phys. Lett. B **643** (2006) 46
- [19] Y. Aoki, S. Borsanyi, S. Durr, Z. Fodor, S. D. Katz, S. Krieg and K. K. Szabo, JHEP **0906** (2009) 088
- [20] S. Borsanyi *et al.* [Wuppertal-Budapest Collaboration], JHEP **1009** (2010) 073
- [21] A. Bazavov *et al.*, Phys. Rev. D **85** (2012) 054503
- [22] R. Bellwied, S. Borsanyi, Z. Fodor, J. Gnther, S. Katz, C. Ratti and K. Szabo, Phys. Lett. B **751** (2015) 559
- [23] P. Cea, L. Cosmai and A. Papa, arXiv:1508.07599 [hep-lat].
- [24] C. Bonati, M. D'Elia, M. Mariti, M. Mesiti, F. Negro and F. Sanfilippo, Phys. Rev. D **92** (2015) 5, 054503
- [25] C. S. Fischer, J. Luecker and C. A. Welzbacher, Phys. Rev. D **90** (2014) 3, 034022
- [26] J. Cleymans, B. Kampfer, M. Kaneta, S. Wheaton and N. Xu, Phys. Rev. C **71** (2005) 054901
- [27] F. Becattini, J. Manninen and M. Gazdzicki, Phys. Rev. C **73** (2006) 044905
- [28] A. Andronic, P. Braun-Munzinger, J. Stachel, Phys. Lett. B **673** (2009) 142 [Phys. Lett. B **678** (2009) 516]
- [29] F. Becattini *et al.* Phys. Rev. Lett. **111** (2013) 082302
- [30] J. Stachel, A. Andronic, P. Braun-Munzinger and K. Redlich, J. Phys. Conf. Ser. **509** (2014) 012019
- [31] A. Andronic, Int. J. Mod. Phys. A **29** (2014) 1430047
- [32] P. Alba *et al.* Phys. Lett. B **738** (2014) 305
- [33] F. Karsch, Central Eur. J. Phys. **10** (2012) 1234
- [34] S. Borsanyi, Z. Fodor, S. D. Katz, S. Krieg, C. Ratti and K. K. Szabo, Phys. Rev. Lett. **111** (2013) 062005
- [35] V. Koch, Chapter of the book "Relativistic Heavy Ion Physics", R. Stock (Ed.), Springer, Heidelberg, 2010, p. 626-652. (Landolt-Boernstein New Series I, v. 23). (ISBN: 978-3-642-01538-0, 978-3-642-01539-7 (eBook)) [arXiv:0810.2520 [nucl-th]].
- [36] V. Skokov, B. Friman and K. Redlich, Phys. Rev. C **88** (2013) 034911
- [37] A. Bzdak and V. Koch, Phys. Rev. C **86** (2012) 044904
- [38] S. Jeon and V. Koch, Phys. Rev. Lett. **85** (2000) 2076
- [39] M. Kitazawa and M. Asakawa, Phys. Rev. C **85** (2012) 021901
- [40] M. Nahrgang, M. Bluhm, P. Alba, R. Bellwied and C. Ratti, Eur. Phys. J. C **75** (2015) 12, 573
- [41] P. Alba, R. Bellwied, M. Bluhm, V. M. Sarti, M. Nahrgang and C. Ratti, Phys. Rev. C **92** (2015) 6, 064910
- [42] F. Becattini, M. Bleicher, T. Kollegger, T. Schuster, J. Steinheimer and R. Stock, Phys. Rev. Lett. **111** (2013) 082302
- [43] S. Borsanyi, Z. Fodor, S. D. Katz, S. Krieg, C. Ratti and K. K. Szabo, Phys. Rev. Lett. **113** (2014) 052301
- [44] L. Adamczyk *et al.* [STAR Collaboration], Phys. Rev. Lett. **112** (2014) 032302
- [45] L. Adamczyk *et al.* [STAR Collaboration], Phys. Rev. Lett. **113** (2014) 092301
- [46] A. Bazavov *et al.*, arXiv:1509.05786 [hep-lat].
- [47] J. Xu, these proceedings.
- [48] R. Preghenella (ALICE), Acta Phys. Polon. B43, 555 (2012).
- [49] M. Floris, Nucl. Phys. A931, 103 (2014).
- [50] F. Becattini, M. Bleicher, T. Kollegger, M. Mitrovski, T. Schuster, and R. Stock, Phys. Rev. C85, 044921 (2012).
- [51] F. Becattini, M. Bleicher, T. Kollegger, T. Schuster, J. Steinheimer, and R. Stock, Phys. Rev. Lett. **111**, 082302 (2013).
- [52] J. Steinheimer, J. Aichelin, and M. Bleicher, Phys. Rev. Lett. **110**, 042501 (2013)
- [53] R. Bellwied, S. Borsanyi, Z. Fodor, S. D. Katz, and C. Ratti, Phys. Rev. Lett. **111**, 202302 (2013).
- [54] A. Bazavov *et al.*, Phys. Rev. Lett. **113**, 072001 (2014).
- [55] J. Noronha-Hostler and C. Greiner, (2014), arXiv:1405.7298 [nucl-th]
- [56] J. Noronha-Hostler and C. Greiner, Nucl. Phys. A931, 1108 (2014), arXiv:1408.0761 [nucl-th].
- [57] S. Chatterjee, R. M. Godbole, and S. Gupta, Phys. Lett. B727, 554 (2013), arXiv:1306.2006 [nucl-th]
- [58] J. Noronha-Hostler, R. Bellwied, J. Gunther, P. Parotto, A. Pasztor, I. Portillo Vazquez and C. Ratti, arXiv:1607.02527 [hep-ph].